INDERSCIENCE PUBLISHERS
Linking academia, business and industry through research

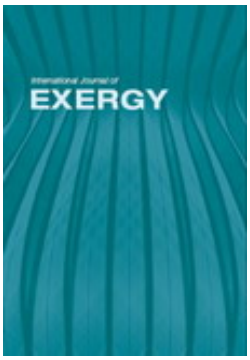

International Journal of Exergy

ISSN online: 1742-8300 - ISSN print: 1742-8297
https://www.inderscience.com/ijex

Investigating the energetic and exergetic performance of a solar based cooling-heating-low temperature refrigeration system

Tawfiq Al-Mughanam, Abdul Khaliq

DOI: 10.1504/IJEX.2025.10068581

Article History:

Received:	30 July 2024
Last revised:	28 October 2024
Accepted:	30 October 2024
Published online:	07 January 2025

Investigating the energetic and exergetic performance of a solar based cooling-heating-low temperature refrigeration system

Tawfiq Al-Mughanam*

Department of Mechanical Engineering,
College of Engineering,
King Faisal University,
380, Al-Ahsa 31982, Saudi Arabia
Email: talmughanam@kfu.edu.sa
*Corresponding author

Abdul Khaliq

Mechanical Engineering Department,
College of Engineering at Yanbu,
Taibah University,
Yanbu Al-Bahr 41911, Saudi Arabia
Email: khaliqsb@gmail.com

Abstract: A novel trigeneration system powered by helically coiled tubes embedded solar collector is proposed. A study using ANSYS-FLUENT simulation was conducted to investigate the impact of coil torsion and coil curvature ratio. The EES software examined the system from energy and exergy perspectives, which showed that coil curvature ratio has positive impact on temperature of solar fluid, whereas coil torsion has negative effect. At 0.032 coil torsion, temperature increased by 28.9% as curvature ratio increased from 0.063 to 0.095 at 1,200 W/m^2. From solar exergy supplied, 13.29% is produced exergy, 1.98% is lost exergy, and 84.73% is the exergy destroyed.

Keywords: helically coiled tubes based heliostat field; trigeneration system; exergetic; transcritical CO_2 refrigeration cycle; low temperature refrigeration.

Reference to this paper should be made as follows: Al-Mughanam, T. and Khaliq, A. (2025) 'Investigating the energetic and exergetic performance of a solar based cooling-heating-low temperature refrigeration system', *Int. J. Exergy*, Vol. 46, No. 1, pp.79–92.

Biographical notes: Tawfiq Al-Mughanam is currently working as an Assistant Professor in the Department of Mechanical Engineering of the College of Engineering at King Faisal University, Kingdom of Saudi Arabia since 2014, He earned his PhD in Thermal-Fluid Science from University of Leeds, Leeds, West Yorkshire, UK in 2013. He has many publications in the area of thermal science and cited by many researchers in the same field.

Abdul Khaliq is currently working as a Professor in the Department of Mechanical Engineering of the College of Engineering at Yanbu of Taibah University, Saudi Arabia. He earned his PhD in Thermal-fluid Engineering from IIT Delhi, India in 2003. He is an eminent authority in the area

'Thermodynamics and Energy'. Large number of research papers in high impact *Journals of International Repute* are credited to his name. A US Patent of Solar Thermal Cooling System is also granted to him as its Principal Inventor. His publications are cited by many preeminent researchers of the area by more than thousand times.

1 Introduction

Utilisation of solar energy for driving the systems which can generate various kinds of outputs (power, heating for industrial use or drying and cold production for refrigeration and air conditioning) can provide a sustainable energy option because such systems are environment-friendly and provide high efficiency (Aghaziarati and Aghdam, 2021; Alharthi et al., 2023; Siddiqui, 2024). Further, production of cooling at two different levels of temperature along with heating using a solar thermal source is quite worth as it provides an opportunity to exploit the close coincidence of observing the high cooling demand for driving the refrigeration and air conditioning units during peak summer periods when highest solar rays are observed (Khaliq et al., 2020; Habib et al., 2023). Integration of organic Rankine cycle (ORC) with absorption refrigeration cycle (ARC) presents an energy-efficient and sustainable solution that can effectively meet the increasing cooling requirements in these hot areas, offering a compelling alternative to traditional cooling systems (Siddiqui and Khan, 2024). In this regard, Grosu et al. (2016) developed a solar-powered system incorporating a tower solar collector with the ORC, utilising the bottoming of ARC. Their exergy-based analysis revealed how the components efficiency affects the overall effectiveness of the proposed system. Eisavi et al. (2018) analysed CCHP system producing power, heat, and cold utilising solar energy. Their system comprised of ORC for electric power, LiBr-H_2O operated absorption machine for cooling production, and heat exchanger for process heating, respectively. Mahdavi et al. (2022) devised a novel solar based trigeneration system consists of a dual-pressure ORC and the cooling cycle for simultaneous generation of cold, heat, and power. They analysed the devised system from energy and exergy viewpoints and obtained the system efficiencies as 20.26% and 15.81%, respectively, at a constant rate of solar radiation (DNI) as 1,000 W/m^2.

Research reported above in regard of the proposal and investigation of solar based systems using ORC reveals that these systems have limitations in their capability to refrigerate the thermal load from (–5°C to 22°C), the range of temperature suitable for refrigeration (–5°C to +5°C) requires for preserving of foodstuffs, veggies, and meats in the cold storages, and air conditioning (15°C to 22°C) for office and residential buildings. Some of the industrial applications such as; buildings climatisation, food processing industry, and dairy plants require combined production of low temperature refrigeration and high temperature heating (Agrawal et al., 2014).

Literature surveyed show that energy and exergy investigations as regards ORC based combined system driven by CSP source for simultaneous production of cooling for space conditioning, high temperature heating, and refrigeration below freezing is very scarce and it is still a topic of further research. This motivates the present research aiming to analyse and develop a novel solar powered system for combined generation of cooling for building air conditioning, low temperature refrigeration for laboratories and

pharmacy, and heating for high temperature user. In this regard, in the present study, a transcritical CO_2 refrigeration cycle, an ORC, a helically coiled tubes embedded central receiver based solar collector, and an absorption chiller are integrated into the devised system.

Figure 1 Schematic diagram of solar powered combined system producing cooling for building air-conditioning, high temperature heating, and low temperature refrigeration (see online version for colours)

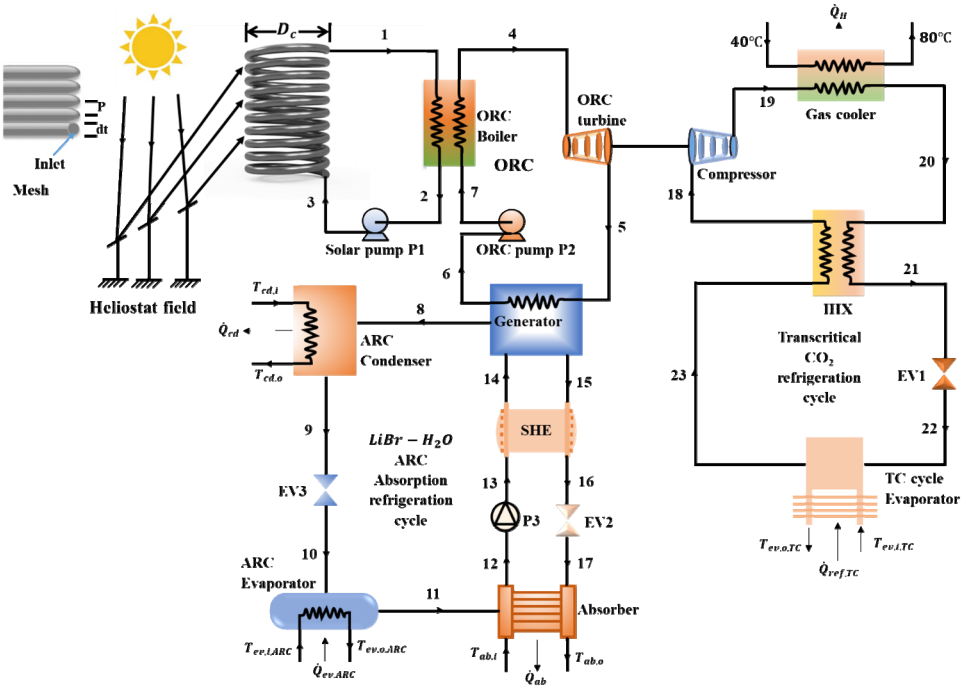

2 System description

Figure 1 illustrates the layout of a proposed solar powered combined energy system. The designed system consists of a tower solar collector, an ORC driven transcritical CO_2 refrigeration cycle and an ARC. The receiver tubes exhibit a helical coiled configuration to facilitate flow. Each coil diameter is D_c, and they are constructed from the tubes of diameter, d, which are organised in the shape of circle. Therminol 66 oil as a medium of heat transfer goes into the tubes and while flowing through the tubes of helically coiled arrangement in the central receiver, absorbing heat from solar radiation reflected by the heliostats onto the receiver's surface, heating up the oil, and its temperature is further increased due to the centrifugal force induced by the curvature of the helical coil, leading to the generation of secondary flow. The selection of Therminol 66 oil as SHTM is due to its offering of the excellent level efficient attributes in facilitating fluid flow within the receiver and absorbing significant heat for vaporising the operating fluid of the ORC. The hot oil (state 1) enters the ORC boiler where it transfers the heat to R113 which is the working fluid of ORC. After being heated in the ORC boiler, the working fluid (state 4)

is fed to the turbine (T) where it is expanded to a low-pressure flow to generate power output ($\dot{W}_{el}$). Finally, the organic substance R113 is pumped back to ORC boiler (state 7). Small portion of power produced by turbine is consumed to drive the pumps and major one is supplied to compressor of transcritical CO_2 refrigeration cycle. The CO_2 as superheated refrigerant (18) is compressed to state (19). The supercritical CO_2 vapor is cooled in the gas cooler (GC) (19–20) using a secondary fluid to achieve high temperature heating while also raising its temperature. Subsequently, the CO_2 undergoes further cooling in the internal heat exchanger (IHX) by heating its saturated vapor (20–21). Finally, the CO_2 is expanded (21) through a throttling valve. The CO_2 is then passed through the evaporator coils (22–23) to produce the desired low temperature refrigeration. The organic substance R113 leaving the ORC turbine passes through the generator (from point 5 to 6) to boil out refrigerant vapour from the weak solution of $LiBr/H_2O$. The solution strong in refrigerant (water) enters the generator at point 14 and after boiling off LiBr and H2O weak solution goes back from point 15 and released the refrigerant at superheated state at 8 which is condensed to saturated liquid state at 9 because external water supplied to condenser carried away the heat of rejection. The refrigerated undergoes an isenthalpic process across the expansion valve (from 9 to 10) till the saturation temperature of refrigerant is reaches out at evaporator pressure. The refrigerant while passing through the evaporator (10 to 11) produces the desired cooling effect. The vaporised refrigerant (state 11) mixes with a weak solution of LiBr and H_2O which is entering the absorber at state 17 where the absorbed heat is rejected via cooling water. This strong solution is then returned to generator at state 14 via solution pump (12 to 13) and through the solution heat exchange in order to raise its pressure and temperature.

3 Main assumptions and the development of mathematical model

Solar collector and the cooling-heating-refrigeration combined system is investigated considering the steady state conditions of all components. In addition, heat loss to ambient and pressure drops are not considered and the flow properties are assumed to be uniform along with the consideration of non-varying isentropic efficiency of power sharing components (Alsaduni and Siddiqui, 2024). The atmospheric pressure P0 and temperature T0 to be taken for the reference-environment were considered as (25°C and 101.325 kPa), respectively.

Each process is modelled through the employment of the equations derived from the laws of mass conservation and energy conservation along with the principle of decrease of exergy.

3.1 Governing equations and mathematical analysis

The investigation uses ANSYS-FLUENT package. Pressure-velocity coupling was done utilising the simple approach, while advanced wall treatment was done nearby. The confined volume approach followed mass, energy, and momentum conservation rules. The grid has wedge and tetrahedral elements, which are illustrated in Figure 1. Convergence is indicated when the normalised residual values for energy, momentum, and continuity are below 10^{-6}, 10^{-5}, and 10^{-5}, respectively. A consistent flowing rate of

mass of 1.1267 kg/s for the diameters of three tube was used to set the Therminol-66 oil temperature boundary conditions at 92°C.

The properties of the coils considered for investigation are taken from the Nada et al. (2018) and they be shown as

Pitch P	40 mm, 50 mm, 60 mm
Diameter of tubes (d_t) used	38 mm, 32 mm, 25 mm
P/(π.Dc)	0.032, 0.04, 0.048
δ = dt/Dc	0.0625, 0.08, 0.095

Grid refinement studies showed that numerical solutions were superior in accurately and consistently capturing crucial parameters near coil walls, strong flows, and temperature gradients. Having a large concentration of cells in these locations was of utmost importance. The oil temperature as it leaves the heat exchanger was found to be dependent on both the number of coil cells and grid size. The oil outlet temperature for a tube with a diameter of 38 mm and a coil diameter (D_c) of 400 mm reached a convergence of 2,181,804 cells (Fouda et al., 2018). The study found that tubes with diameters of 25 mm and 32 mm reached convergence at cell counts of 2,078,747 and 1,944,221, respectively. (Elattar et al., 2018) verified the precision of their CFD models for laminar flow in helical-coiled tubes using the same experimental data. The research looked at the flow of Newtonian fluids, which are solid and cannot be squished. It did not look at how gravity affects the transfer of heat. Cartesian dimensions were used to find the equations for energy, continuity, and momentum that describe how the temperature spreads in the spiral coil (Elattar et al., 2018; Nada et al., 2018).

$$\frac{\partial}{\partial x_i}(\rho U_i) = 0 \tag{1}$$

$$\frac{\partial}{\partial x_i}(\rho U_j U_i) = \frac{\partial}{\partial x_i}\left(\mu \frac{\partial U_i}{\partial x_i}\right) - \frac{-\partial P}{\partial x_i} \tag{2}$$

$$\frac{\partial}{\partial x_i}(\rho C_p U_j T) = \frac{\partial}{\partial x_i}\left(k \frac{\partial T}{\partial x_i}\right) \tag{3}$$

where T and U_i denote the temperature and velocity in the i direction as they evolve with time. The variables P, μ, C_p, k, and ρ stand for thermodynamic pressure, viscosity, heat capacity, thermal conductivity, and density.

The calculation of heat transfer rate Q from oil flow is determined by using the balance of energy equation in the following manner:

The determination of the rate of heat transfer Q from oil flow is calculated through the application of the energy balance equation in the subsequent manner:

$$Q = q'' A_h = \dot{m}_{SHTF} C_p (T_{SHTF,o} - T_{SHTF,i}) \tag{4}$$

where, q'' denotes the coil's outer surface is anticipated to experience a constant heat flux. $T_{SHTF,i}$ and $T_{SHTF,o}$ represent the average inlet and outlet temperatures of the oil (SHTF) respectively. C_p represents the oil's specific heat and $m_{\dot{S}HTF}$ denotes the flowing rate of mass of oil.

3.2 Analyses based on energy and exergy

The schematic of the cycle described in Section 2 is analysed using the first and second laws of thermodynamics to assess the performance of the solar-powered cooling system, which provides cooling for air conditioning, refrigeration, and deep freezing, simultaneously (Rabbani et al., 2015; Grosu et al., 2016).

The mathematical model for energy analysis of the sub-system is derived after applying first law of thermodynamics to process under the assumptions taken above, delivers the equation below

$$\sum \dot{Q} - \sum \dot{W} + \sum \dot{m}_i h_i - \sum \dot{m}_o h_o = 0 \tag{5}$$

The energy and exergy equations for the ORC were considered in line described by Grosu et al. (2016). The behaviour revealed from the application of the balance of concentration of LiBr-H_2O and its energy balance over the components presented by Tausif et al. (2022) were adopted for the energetic and exergetic evaluation of LiBr-H_2O operated ARC, and for the assessment of cooling-heating CO_2 operated transcritical refrigeration cycle the expressions resulted from the study of Khaliq (2015) for the components of proposed system were considered.

The mathematical formulation of exergy can be described as follows. The general equation for balance of exergy for the control volume following the steady-state process can be presented as (Al Mughanam and Khaliq, 2024)

$$\dot{E}x_{in} - \dot{E}x_{out} = \dot{E}x_{,D} \tag{6}$$

where $\dot{E}x_{in}$ and $\dot{E}x_{out}$ denote exergy rates at the input and output of the control volume, respectively. The exergy destruction rate is denoted by $\dot{E}x_{,D}$.

The exergy rate $(\dot{E}x)$ can be expressed as:

$$\dot{E}x = \dot{E}x_Q + \dot{E}x_W + \dot{E}x_{mass} \tag{7}$$

The terms $\dot{E}x_Q$ and $\dot{E}x_W$ are used to denote the exergy transfer rates resulting from interaction with heat and work at the system boundary, respectively, whereas $\dot{E}x_{mass}$ denotes the exergy transfer rate by means of mass transfer through the boundary.

3.3 Overall performance evaluation of the combined cooling-heating-low temperature refrigeration system

To estimate the performance of a presented solar powered trigeneration system from thermodynamic point of views, the parameters considered to indicate the system performance were: energy efficiency or first law efficiency which govern the ratio of energetic output desired from the system to the energy required can be given as

$$\eta_{I,Trigen} = \frac{\dot{Q}ev + \dot{Q}_H + \dot{Q}_{ref}}{\dot{Q}_{solar}} \tag{8}$$

where, $\dot{Q}_{ev}$ denotes the cooling produced by evaporator of ARC, $\dot{Q}_H$ represents the rate of heating produced by gas cooler, and $\dot{Q}_{ref}$ is the rate of low temperature refrigeration

produced by the evaporator transcritical CO_2 cycle, $\dot{Q}_{solar}$ is the heat accompanied by solar rays which is a primary input energy to drive the combined system.

The efficiency of combined system based on energy which is shown in equation (8) estimate the overall performance and unable to signify the thermodynamic losses occurs in the process. Second law application reveals the losses occurred in the system converting the energy supplied to useful energy products.

The ratio of exergy accompanied by energetic gain to the exergy supplied is termed as the exergetic efficiency or second law-based efficiency. When the type of energy supplied to the system is solar thermal then the exergy efficiency appears as a need to incorporate in analysis because in such situations, rest portion of solar fluid is reintroduced to the receiver rather than being dissipated to the atmosphere. Therefore, exergy efficiency pertaining to system operating in trigeneration mode to produce (electricity, process heat, and refrigeration) can be defined as

$$\eta_{II,Trigen} = \frac{\dot{E}_{x,ev} + \dot{E}_{x,H} + \dot{E}_{x,ref}}{\dot{E}_{x,solar}} \tag{9}$$

where $\dot{E}_{x,ev}$ denotes the cooling exergy rate and hence it is a change in refrigerant's exergy found in the evaporator of ARC, $\dot{E}_{x,H}$ is the rate of heating exergy produced by gas cooler, and $\dot{E}_{x,ref}$ is the exergy accompanied by rate of low temperature refrigeration produced by the evaporator of transcritical CO_2 refrigeration cycle. The total exergy associated with the solar irradiation arrived on the heliostat mirror surface can be presented as

$$\dot{E}_{x,solar} = \dot{Q}_{solar}\left(1 - \frac{T_o}{T_s}\right) \tag{10}$$

where, T_s represents the temperature of Sun which is taken from Rabbani et al. (2015), Aghaziarati and Aghdam (2021), and Khaliq et al. (2020) and T_0 is the atmospheric temperature. $\dot{Q}_{solar}$ is the heat associated with solar rays arrives at collector.

Detail of the energy and exergy equations pertaining to formulation of thermodynamic model for the heliostat based central receiver which drives the proposed combined system can be determined in the references (Rabbani et al., 2015; Khaliq, 2015).

4 Results and discussion

4.1 Validation

The results for the tower-solar collector are compared with those presented by previous study (Eisavi et al., 2018). For the use of solar heat transfer fluid of Therminol-66 in the concentrated solar power source, the results obtained from the current model for the system producing cooling and heating shows the trend of decreasing with the increase of the pinch point temperature of ORC. The values obtained for the cooling and heating outputs as well as the values of cooling and heating exergies are in good agreement with the results reported by Eisavi et al., 2018). A little deviation is found due to the use of different solar collector technologies between the two studies.

The system devised in this study was examined from energy and exergy perspectives using an EES software (Klein, 2012). The distribution of energy from solar rays and solar exergy input to a combined system, focusing on output energy, losses to the environment, exergy delivered, exergy destroyed in the components, and exergy loss through heat dissipation to the atmosphere. The impact of coil torsion and coil curvature ratio is observed on the variation of temperature and pressure of solar fluid (oil) flows in coils embedded in receiver to convert solar radiation into heat. Further, the cooling capacity, high temperature heating output, low temperature refrigeration effect, cooling exergy, heating exergy, refrigeration exergy, and the energetic and exergetic efficiencies of the combined mode cycle by changing the solar flux and pinch point temperature difference of the ORC boiler.

The baseline operative conditions considered for the energetic and exergetic investigation of the proposed system were taken from the literature. The parameters related to solar irradiance and the solar collector are taken from Fouda et al. (2018) and the input parameters for conducting the analysis of ORC coupled to transcritical CO_2 cycle and LiBr-H_2O operated ARC were taken from Khaliq, 2015.

The input parameters taken for conducting the energetic and exergetic evaluation of the combined system are as follows:

Coil diameter 250 mm, inlet temperature of oil 92°C, Apparent Sun temperature 4,800°C, Solar flux 800 Wm^2, heliostat field area 5,000 m^2, isentropic efficiency of ORC turbine 85%, isentropic efficiency of ORC turbine 80%, operating fluid for ORC R113, ORC turbine inlet pressure 2,200 kPa, efficiency of ORC boiler 100%, effectiveness of SHE 70%, efficiency of solution pump 95%, ARC evaporator temperature 10°C, high temperature heating produced by gas cooler 80°C, transcritical CO_2 refrigeration cycle evaporator temperature –20°C, Absorber and condenser temperature 35°C, isentropic efficiency of compressor 90%.

The torsional deformation of the coil has an impact on the temperature of the oil produced by three distinct degrees of coil torsion. The higher coil torsion was responsible for the decrease in oil outlet temperature that was observed, as can be depicted in Figure 2(a). The highest decrease in outlet temperature occurs during periods of low radiation intensity (850 W/m^2), while the curvature ratio remains consistent. This is the case when the outlet temperature continues to fall. According to the data, increasing the coil torsion from 0.032 to 0.048 would result in percentage drops of 2%, 7 %, and 4 % for curvature ratios, which are 0.063, 0.08, and 0.095, respectively. This is based on the investigation that was conducted at a DNI of 1,200 W/m^2. The decrease in torsion leads to a decrease in secondary flow and a reduction in the amount of fluid intermingling, both of which contribute to the preservation of the velocity and temperature boundary layers throughout the process.

Using incoming radiation (DNI = 1,200 W/m^2) and different curvature ratios, the temperature of the Syltherm oil flowing out of the investigated coil torsions changes. Figure 2(b) illustrates the impact of the coil curvature ratio on the output temperature of Syltherm oil, displaying the relationship between these two variables. The data is shown for different incoming radiation levels. Evidence suggests that, under all conditions, a higher output temperature is directly proportional to a higher curvature ratio. As the curvature ratio increases, the results show that the outflow temperature increases significantly. At 0.032 coil torsion, the temperature increased by 28.9% as the curvature ratio increased from 0.063 to 0.095 at 1,200 W/m^2. At 1,200 W/m^2, the curvature ratio increased from 0.063 to 0.095, leading to a maximum temperature increase of about

37.5% as coil torsion increases. The improvement in secondary flow efficiency and the consequent enhancement in centrifugal force are the reasons for this. Thus, the curvature ratio is more important than the coil torsion.

Figure 2 (a) Impact of coil torsion on curvature ratio's outlet temperature and (b) the variation of curvature ratio on the outlet temperature (see online version for colours)

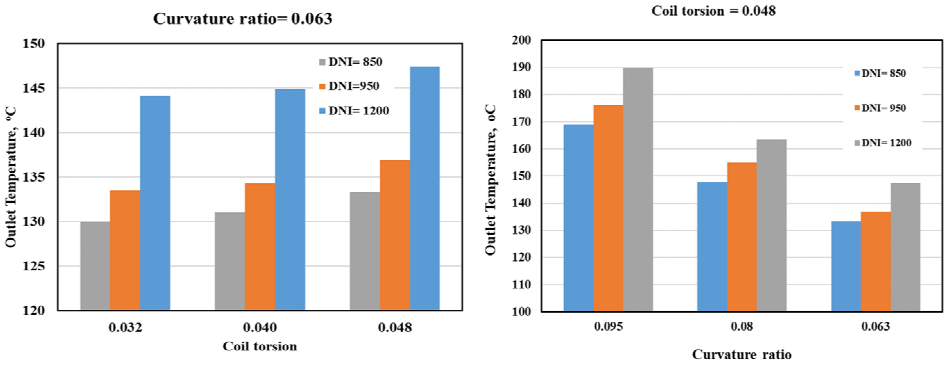

(a) (b)

The impact of the variation of solar flux is examined on the generation of cooling energy, cooling exergy, low temperature refrigeration, refrigeration exergy, high temperature heating, heating exergy as well as on the energetic and exergetic efficiencies of the combined energy system as shown in Figure 3. According to Figure 3(a), the cooling output, heating output, and the capacity of low temperature refrigeration are increased considerably as solar flux goes up. The larger solar flux reaching the heliostat results in a higher solar intensity being reflected onto the receiver. This elevated solar intensity results in a higher temperature of the oil as it passes through the receiver tubes. When applying an energy balance to the ORC boiler given the assumed conditions, it becomes evident that the introduction of this high-temperature oil into the boiler causes an increase in the enthalpy of the ORC working fluid. This expanded working fluid then drives the power turbine, ultimately increasing the overall turbine power output. Since power generated by turbine is the prime mover to drive the transcritical (TC) CO_2 cycle producing heating and cooling, therefore, increase in turbine power increases the amount of power supplied to compressors which in turn increase the low temperature refrigeration effect at the evaporator and high temperature heating output of the gas cooler. Additionally, as the high-temperature HTF oil flows through the generator of ARC, it leads to an increase in the flowing rate of mass of the working fluid (water), thereby enhancing the cooling rate at the bottoming cycle's evaporator. The cooling output, heating output, and low temperature refrigeration effect delivered by combined system were found to increase from 504.81 kW to 594.86 kW, 306.47 kW to 382.79 kW, and 202.34 kw to 281.96 kW, respectively, when the solar flux is raised from 600 W/m^2 to 1000 W/m^2. The exergy accompanied by cooling, heating, and refrigeration effects produced by combined system is appears to be significantly less compared to energy outputs. The low temperature refrigeration exergy and heating exergy produced by TC CO_2 cycle are raised from 15.69 kW to 23.65 kW and 31.24 kW to 47.75 kW, the cooling exergy goes up from 36.83 kw to 52.89 kw when the solar flux increases from 600 W/m^2 to 1,000 W/m^2 as it is observed from Figure 3(b).

The energy and exergy efficiencies of combined system were also computed and a considerable enhancement in system efficiencies is found at the rise of solar flux as shown in Figure 4(a). This attributes to the fact that higher solar flux causes a significant rise in ORC turbine power which leads to a simultaneous increase in the amount of heating output and low temperature refrigeration capacity, and large solar flux also results in increase of heat offered to generator of ARC which leads to increase of cooling capacity. Since overall energy output is increasing for a fixed energy input, therefore, the energy efficiency is found to be increasing and for the similar reasons a significant gain is obtained in the exergy efficiency of combined system. The increasing rate in the efficiencies based on exergy and energy is similar but the exergy efficiency level is found to be less than the energy-based efficiency of the system at a fixed value of solar flux. This difference appears because of the greater difference between the values of the energy, and the exergy accompanied by the cooling capacity, low temperature refrigeration effect, and high temperature heating. At the base simulation condition, the energetic and exergetic efficiencies of combined system are found 50.49% and 10.79%, respectively.

Figure 3 Effect of increase of solar flux on (a) cooling for building air conditioning, high temperature heating output, and low temperature refrigeration output and (b) cooling exergy, heating exergy, and low temperature refrigeration exergy produced by combined system (see online version for colours)

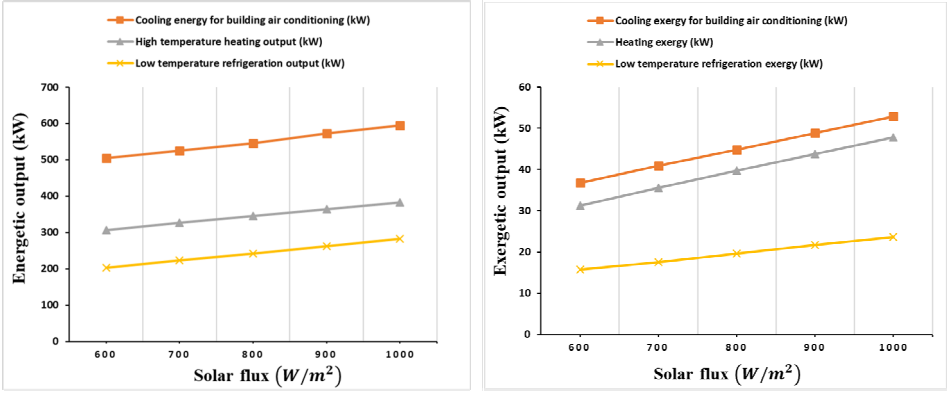

(a) (b)

Figure 4(b) shows the variation of combined system's energetic and exergetic outputs produces as cooling energy, heating output, refrigeration effect, cooling exergy, heating exergy, and the refrigeration exergy as ORC boiler pinch point temperature (TPP) changes. It is found that the high temperature heating and low temperature refrigeration outputs drops from 378.14 kW to 310.74 kW and 277.46 kW to 206.14 kW, respectively as TPP changes from 5°C to 25°C. The reason for this decline is the decrease in the rate of heat input to ORC boiler, which leads a decline in the turbine intake temperature and subsequently a reduction in turbine power output means a decrease in power supplied to compressor which in turn reduces the heating and refrigeration outputs of TC CO_2 cycle. Also, as stated earlier, when ORC boiler temperature rises, the heat offered to the ARC generator declines which leads to decrease the cooling produced by evaporator of ARC which causes a significant decline in the cooling capacity of ARC from 589.76 kW to

510.17 kW. Figure 4(b) also presents the impact of varying the TPP on exergetic output of the system. With the promotion of TPP from 5°C to 25°C the cooling exergy, heating exergy, and low temperature refrigeration exergy are seen to decrease. The heating exergy and refrigeration exergy are found to decline from 47.14 kW to 31.14 kW and from 23.19 kW to 15.12 kW, respectively. In addition, increase of TPP from 5°C to 25°C reduces the cooling exergy from 52.13 kW to 36.17 kW.

Discretising the solar energy supplies to drive the combined system is illustrated in Figure 5(a). It is shown that 62% of solar energy supplied is delivered as energetic output (cooling for building air conditioning 31.45%, high temperature heating output 23.94%, and low temperature refrigeration effect 10.74%). Remaining 33.87% of solar energy is dissipated as thermal exhaust discarded to atmosphere from the solar collector, and the absorber and condenser of ARC.

Figure 4 (a) Impact of changing the solar fluid temperature on energetic and exergetic efficiency of combined system and (b) the impact of changing the pinch point temperature of ORC boiler on cooling for building air conditioning, heating output, and refrigeration effect from the combined system (see online version for colours)

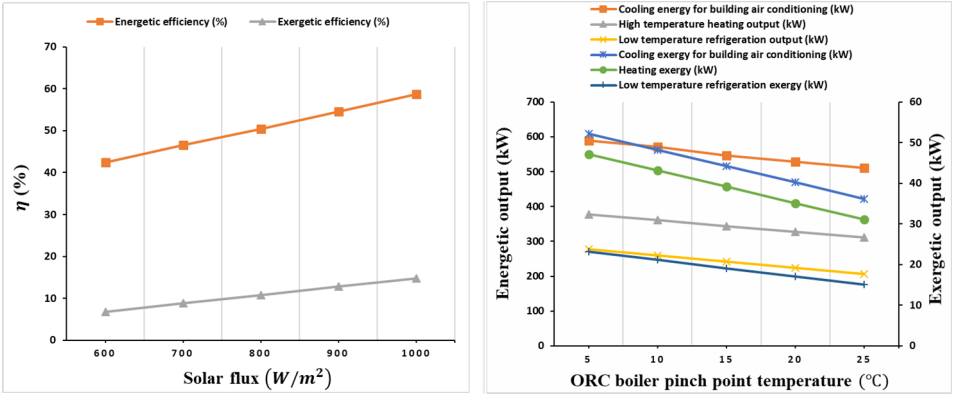

(a) (b)

The application of the principle of decrease of exergy to the developed solar driven cooling-heating-refrigeration system resulted in the distribution of solar exergy input into cooling exergy, refrigeration exergy, and heating exergy, and exergy loss and also the exergy destructed due to entropy creation in the components. In this context, percentage of exergy of solar input transformed into the exergy destroyed, exergy loss, and the exergy delivered by combined system is evaluated and shown in Figure 5(b).

In the proposed combined system, from 100% radiative solar exergy supplied, 13.29% was transformed into output of exergy (cooling exergy 5.46%, heating exergy 4.96%, and refrigeration exergy 2.87%), 1.98% is lost through heat rejection to the atmosphere at the solar collector and various heat exchangers of the system, and the remaining 84.73% is destroyed due to thermodynamic irreversibilities. The study found that the receiver and heliostat in a trigeneration system waste a lot of solar energy. This means they need special attention to improve the system's performance. The receiver loses a lot of energy because it absorbs high-quality solar energy at a lower temperature, leading to increased entropy and greater thermodynamic irreversibility. Apart from heliostat and receiver, ORC boiler also shows significant exergy losses due to the

generation of entropy associated with heat transfer occurs between the Thermino-66 oil and the ORC working fluid (R113). Exergy dissipated in rest of the components of the system; the turbine, ORC pump cycle, gas cooler and evaporator of TC CO_2 cycle, and in ARC sub-systems was found as the little percentage of the solar exergy supplied to system proposed, thus, percentage of exergy destruction for these sub-systems is not depicted.

Figure 5 (a) Breaking down of solar energy input into energy produced as cooling, heating, refrigeration, and energy lost (b) breaking down of solar exergy input into energy produced as cooling exergy, heating exergy, refrigeration exergy loss, and exergy destroyed (see online version for colours)

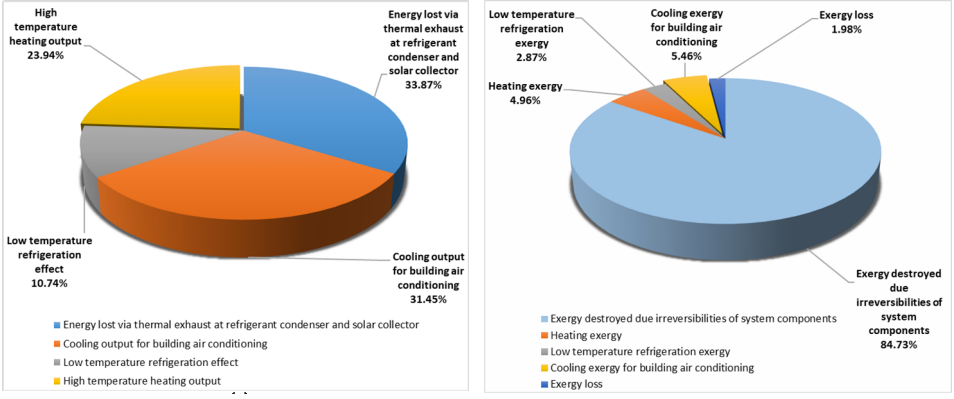

(a) (b)

5 Conclusions

A new solar tower based integrated system for combined production of cooling, high temperature heating, and low temperature refrigeration is developed. The energetic and exergetic investigations of a combined system comprises of a helically coiled tubes embedded central receiver of a heliostat field, an ORC driven TC CO_2 refrigeration cycle, and an ARC are conducted. The effects of changing system operating conditions on the efficiencies of system are studied. Promotion of coil curvature ratio shows a positive impact on temperature of solar fluid, whereas coil torsion has negative effect. At 0.032 coil torsion, oil temperature is increased by 28.9% when curvature ratio is increased from 0.063 to 0.095 at 1,200 W/m^2. As the solar flux is increased, the cooling output, heating output, and low temperature refrigeration produced by the system rises considerably. Further, it is shown that 62% of solar energy supply is delivered as energetic output (cooling effect 31.45%, high temperature heating output 23.94%, and low temperature refrigeration effect 10.74%). Remaining 33.87% of solar energy is lost to environment. Solar exergy distribution reveals, 13.29% is the produced exergy (cooling exergy 5.46%, heating exergy 4.96%, and refrigeration exergy 2.87%), 1.98% is the exergy loss, the remaining 84.73% is destroyed due to thermodynamic irreversibilities in the system.

Acknowledgements

The authors acknowledge the Deanship of Scientific Research, Vice Presidency for Graduate Studies and Scientific Research at King Faisal University, Saudi Arabia, for financial support under the annual funding track [KFU242285].

References

Aghaziarati, Z. and Aghdam, A.H. (2021) 'Thermoeconomic analysis of a novel combined cooling, heating and power system based on solar organic Rankine cycle and cascade refrigeration cycle, renew', *Energy*, Vol. 164, pp.1267–1283.

Agrawal, S.K., Kumar, R. and Khaliq, A. (2014) 'First and second law investigation of a new solar assisted thermodynamic cycle for triple effect refrigeration', *International Journal of Energy Research*, Vol. 38, No. 2, pp.162–173.

Al Mughanam, T. and Khaliq, A. (2024) 'Energetic and exergetic assessments of a new solar energy based trigeneration system for cleaner production of hydrogen, refrigeration, and electricity', *International Journal of Exergy*, Vol. 43, No. 2, pp.177–194.

Alharthi, M.A., Khaliq, A., Alqaed, S. and Almehmadi, F. (2023) 'Investigation of new combined cooling, heating and power system based on solar thermal power cycle and single-double-effect refrigeration cycle', *Energy Reports*, Vol. 9, Supplement 4, pp.289–309.

Alsaduni, I. and Siddiqui, M.A. (2024) 'Thermodynamic and economic evaluation of a developed solar-driven system for efficient production of power and cooling', *Int. J. Exergy*, Vol. 45, Nos. 3–4, pp.219–235.

Eisavi, B., Khalilarya, S., Chitsaz, A. and Rosen, M.A. (2018) 'Thermodynamic analysis of a novel combined cooling, heating and power system driven by solar energy', *Applied Thermal Engineering*, Vol. 129, pp.1219–1229.

Elattar, H.F., Fouda, A., Nada, S.A., Refaey, H.A. and Al-Zahrani, A. (2018) 'Thermal and hydraulic numerical study for a novel multi tubes in tube helically coiled heat exchangers: effects of operating/geometric parameters', *Int. J. Therm. Sci*., Vol. 128, pp.70–83.

Fouda, A., Nada, S.A., Elattar, H.F., Refaey, H.A., Bin-Mahfouz, A.S. (2018) 'Thermal performance modeling of turbulent flow in multi tube in tube helically coiled heat exchangers', *Int. Journal of Mechanical Sciences*, Vol. 135, pp.621–638.

Grosu, L., Marin, A., Dobrovicescu, A. and Oueiros-code, D. (2016) 'Exergy analysis of a solar combined cycle: organic Rankine cycle and absorption cooling system', *Int. J. of Energy and Environmental Engineering*, Vol. 7, pp.449–459.

Habib, M.A., Haque, M.A., Imteyaz, B., Husain, M. and Abdelnaby, M.M. (2023) 'Potential of integrating solar energy into systems thermal power generation, cooling-refrigeration, hydrogen production, and carbon capture', *ASME J. Energy Resour. Technol*., Vol. 145, No. 11, p.110801.

Khaliq, A. (2015) 'A theoretical study on a novel solar based integrated system for simultaneous production of cooling and heating', *Int. J. Refrigeration*, Vol. 52, pp.66–82.

Khaliq, A., Alharthi, M.A., Alqaed, S., Mokheimer, E.M.A. and Kumar, R. (2020) 'Analysis and assessment of tower solar collector driven trigeneration system', *J. Solar Energy Engineering*, Vol. 142, No. 5, p.51003-1.

Klein, S.A. (2012) 'Engineering Equation Solver (EES) for Microsoft Windows operating systems: Academic professional version', *F-chart Software*, Medison, W.I. [online] http://www.fchart.com (accessed 15 June 2024).

Mahdavi, N., Ghaebi, H. and Minaei, A. (2022) 'Proposal and multi-aspect assessment of a novel solar-based trigeneration system; investigation of zeotropic mixture's utilization', *Appl. Therm. Eng*., Vol. 206, p.118110.

Nada, S.A., Elattar, H.F., Fouda, A. and Refaey, H.A. (2018) 'Numerical investigation of heat transfer in annulus laminar flow of multi tubes-in-tube helical coil', *Heat Mass Transf.*, Vol. 54, No. 3, pp.715–726.

Rabbani, M., Ratlamwala, T.A.H. and Dincer, I. (2015) 'Transient energy and exergy analyses of a solar based integrated system', *ASME J. Sol. Energy Eng.*, Vol. 137, No. 1, p.11010-(1-8).

Siddiqui, M. A. (2024) 'thermodynamic analysis and performance assessment of a novel solar-based multigeneration system for electricity, cooling, heating, and freshwater production', *ASME. J. Sol. Energy Eng.*, Vol. 146, No. 2, p.21007.

Siddiqui, M.A. and Khan, T.M.Y. (2024) 'Thermodynamic analysis of solar tower collector integrated with steam Rankine cycle, organic Rankine cycle and absorption refrigeration cycles for cogeneration of power and cooling', *Int. J. Exergy*, Vol. 43, No. 3, pp.229–250.

Tausif, A., Azhar, M., Sinha, M.K., Meraj, M., Mahbubul, I.M., Ahmad, A. (2022) 'Energy analysis of lithium bromide-water and lithium chloride-water based single effect vapour absorption refrigeration system: a comparison study', *Cleaner Engineering and Technology*, Vol. 7, p.100432.